A Kinetic Study on $LaFeO_{3-\delta}$ Preparation with Solid-state Reaction Technique

Baijun Yan*, Qin Feng, Jianhua Liu and Kuo Chih Chou

Dept. Physical Chemistry of Metallurgy, University of Science and Technology Beijing, Beijing 100083, China

(Received March 27, 2009)

ABSTRACT

The present paper describes the kinetic study on the formation of $LaFeO_{3-\delta}$ with solid-state reaction technique. Pellet samples formed using $La_2O_3$and Fe_2O_3 powdered mixture were isothermally calcined to produce the $LaFeO_{3-\delta}$ compound at temperatures, 1273, 1323, 1373 and 1423K respectively. Powder XRD measurements were adopted to determine the phase composition of air-quenched pellets quantitatively. The results showed that there was no intermediate phase produced between $La_2O_3$and Fe_2O_3 during the $LaFeO_{3-\delta}$ formation and the process was controlled by 3D diffusion of solid-state ions. The apparent activation energy values calculated using Jander and Dunwald-Wagner equation were 282.4 and 296.8 kJ/mol respectively. The analysis showed that the oxygen ion diffusion may not be the rate controlling step, lanthanum ion diffusion may control the process of the $LaFeO_{3-\delta}$ formation.

1. INTRODUCTION

$LaFeO_{3-\delta}$ based materials, as ionic and electronic mixed conductors, possess orthorhombic-distorted perovksite structure /1,2/. Cobalt and strontium doped lanthanum ferrites have been used as cathode material in SOFC /3,4/, oxygen separation membranes /5,6/. Li and Ag doped lanthanum ferrites can be used as catalysts for oxidation reactions /7,8/. Studies regarding $LaFeO_{3-\delta}$ based materials have been found mainly focusing on the structure, thermal expansion, electrical conductivities /3,6/, as well as the synthesizing techniques /9-12/. Though wet chemical routes are reported to be preferable for producing compounds of rare-earth oxide composites with higher chemical activity, still the conventional solid-state reaction approach is regarded as effective for its simplicity, flexibility and convenience in chemical composition control /10, 13-14/. This is particularly true in new materials developments, and for producing large amounts of the materials. It is certain that $LaFeO_{3-\delta}$ can be synthesized using solid oxides-reaction technique in air-atmosphere from thermodynamic consideration. Up to now, however, no publications have been found in literature dealing with the process kinetics for the formation of un-doped or doped lanthanum ferrites. The present paper describes kinetic aspect in isothermally synthesizing $LaFeO_{3-\delta}$ using solid-state reaction technique. The present study is a part of the study sequence on LaMe(Me=Co, Mn, Fe)O_3 based materials /13, 15-19/ carried out in the present group.

2. EXPERIMENTAL

2. 1 Sample preparation

La_2O_3 (purity 99.9%) and Fe_2O_3 (99%) were used for synthesizing $LaFeO_{3-\delta}$. Before weighing, La_2O_3 reagent had been pre-heated at 1223K for 3 hrs to remove the absorbed moisture and carbon dioxide. The powder oxides with required molar ratio were thoroughly mixed in a PVA jar with ethanol for 3.5 hrs

*Corresponding author: E-mail address: baijunyan@metall.ustb.edu.cn;
Tel: +86 (10)6233 2732, fax: +86 (10)6232 7283,

after weighting. The average diameter of the powder after mixing was about 2 μm. The powder mixture was dried around 348K, and pressed with a pressure of 150 MPa into pellets. The pellets were 13.2 mm in diameter and 1.4 mm in thickness, and each was 0.6 gram in weight. Three pellets were put in a crucible and the crucible was positioned at the even-temperature zone in a vertical resistance furnace to calcine at a pre-determined constant temperature for a pre-determined period of time.

For the kinetic investigation of the formation, isothermal calcinations of the pellets were carried out at 1273,1323, 1373 and 1423K respectively. For each temperature, continuous calcinations lasted for different time periods. After heating, samples were taken out from the furnace and quenched in air, and then grounded in an agate mortar to ensure the mean particle diameter less than 10 μm for powder XRD measurement.

In order to get a mono-perovskite phase without impurities, the pellets were heated at 1473 K in air-atmosphere for 8 hours. Then they were taken out, quenched in air, ground and pelletized again. The pellets were heated in air at 1473 K for the second 8 hours, followed with quenching and grinding again.

2.2 Sample analysis

Room temperature XRD measurements were performed in a D/MAX 2500-RB12 kW X-ray diffractometer for phase identification of the calcined samples. The parameters used in the measurements were as follows: Cu Kα radiation (40kV), 2θ range between 10° and 90°, step length of 0.01° and a rate of 1°/min. The intensity decrease for the characteristic XRD peaks of Fe_2O_3 with the heating time at all the experimental temperatures could be seen from the obtained XRD patterns.

An approach proposed by Chung /20/ was employed in the XRD measurement for the quantitative analysis of the phase composition of the pellets after calcination. To apply such an approach, a carefully chosen matrix–flushing agent (also termed as internal standard) is needed to mix with the sample powder to form a so-called composite sample in a preliminarily specified mass ratio. The composite samples, not the calcined sample powder directly, were used for room temperature XRD measurements. In the present study, silver powder was selected as the matrix-flushing agent. This selection was due to its chemical and structural stability, also its absorbing coefficient, 2341.72 cm^{-1}, not very much larger than the value of 1214.47 cm^{-1} for Fe_2O_3. The mass ratio of silver to the sample powder was taken as much as one third. The silver powder (99.99%) and the sample powder were thoroughly mixed in an agate mortar with alcohol as mixing medium and dried to form the composite sample.

For quantitative XRD analysis of composite samples, the measurements were carried out using the same X-ray diffractometer mentioned above with Cu Kα radiation (40kV, 250mA). Other parameters involved the receiving slit 0.15mm, divergence slit 0.1°, scatter slit 0.1°, and graphic crystal monochromator. The 2θ scanning was in a range between 30° and 40° with steps of 0.01° and scanning rate of 1°/min. As mentioned earlier, using room temperature XRD measurements with the matrix-flushing approach proposed by Chung /20/, the fractional conversion to Fe_2O_3 in pellets quenched after heating could be determined. Figure 1 shows the XRD pattern of the mixture of Ag and Fe_2O_3 with mass ratio of 1:1. It can be seen that no overlap between the most intensive peak for sliver and its neighboring Fe_2O_3 peaks, and the intensity ration between the peak and Ag and the peaks of Fe_2O_3 are comparable. In this case, the intensities of peaks:(104) for Fe_2O_3 and (111) for silver were determined to calculate mass fraction values of Fe_2O_3 in the composite samples.

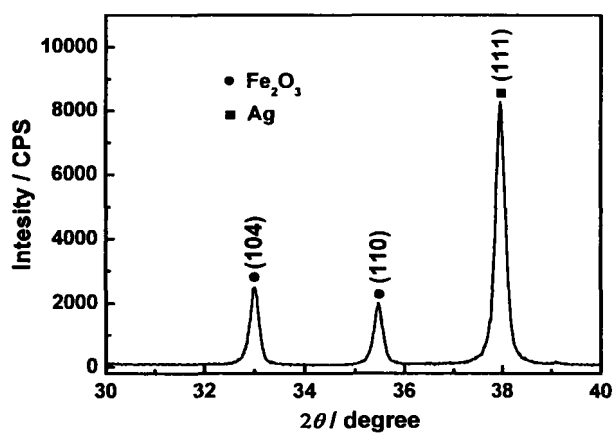

Fig. 1: The XRD pattern of $FeB_{2B}OB_{3B}$ and Ag powder mixture with their mass ratio of 1:1

3. RESULTS

Figure 2 shows the XRD pattern of the mono- and orthorhombic-distorted perovskite phase of $LaFeO_{3-\delta}$ obtained after two periods of calcinations totally for 16 hours for the pellet shaped oxide mixture. From the measured XRD data in this figure, the following lattice parameters calculated using Teror code were obtained: a=0.5553nm, b=0.5561nm, c=0.7842nm, V=0.2422 nm^3. Only the parameter c (and V) is slightly lower than the data reported /1,2/.

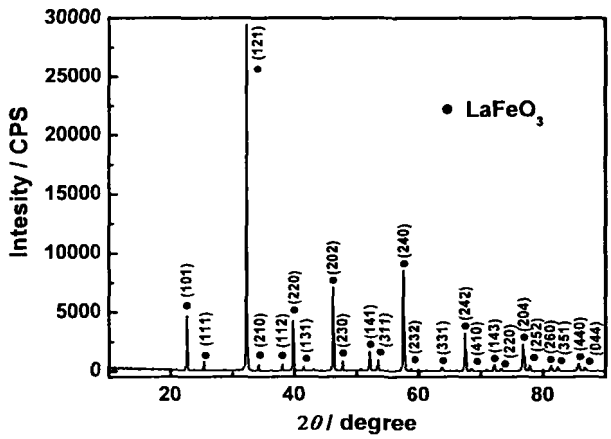

Fig. 2: The XRD pattern of pure $LaFeO_{3-\delta}$ obtained after two calcinations for 16 hrs totally at 1473K

According to the method proposed by Chung /20/, the following equation was used for the conversion from peak intensities mentioned above to the mass fraction of Fe_2O_3 in the composite samples.

$$x_{Fe_2O_3} = K^{Ag}_{Fe_2O_3} \frac{I^{(104)}_{Fe_2O_3}}{I^{(111)}_{Ag}} \frac{x_{Ag}}{1-x_{Ag}} \tag{1}$$

where $I^{(104)}_{Fe_2O_3}$ and $I^{(111)}_{Ag}$ respectively stand for the intensities of peak (104) for Fe_2O_3 and peak (111) for silver in a composite sample, $x_{Fe_2O_3}$ and x_{Ag} - the mass fraction of Fe_2O_3 and silver. $K^{Ag}_{Fe_2O_3}$ is the intensity ratio of peak (111) for silver to that of peak (104) for Fe_2O_3 in the sample containing both silver and Fe_2O_3 with mass ratio of 1:1. $K^{Ag}_{Fe_2O_3}$ determined was as large as 3.328 in the present study.

Figure 3(a) through (d) shows XRD patterns from 32.5° to 40° for the composite samples calcined at 1273, 1323, 1373, 1423K. The measured peak intensity data for Fe_2O_3 and silver for composite samples corresponding to different temperatures and heating time periods were used to convert to mass fraction of Fe_2O_3, then to fractional conversion for the reactant in the pellet samples. These fractional conversion data are listed in **Table 1**.

In a solid-state reaction, the solid product formation process usually involves the following steps: the nuclear formation and growth, the movement of phase (reacting interface) boundary and the diffusion of reactant species through the product layer. The kinetic equations for various rate-controlling steps have been well established. The mechanism of nuclear formation and growth controlling, or the movement of phase boundary controlling often occurs at initial stage, and at relatively lower temperature. At high temperature, usually diffusion is the rate-controlling step for its low rate. In the present study, the commonly used kinetic equations were employed to fit experimental data. The fitting using equations corresponding to 3D solid ions diffusion produced much better precision among others. These include the uses of the Jander /21/, Ginstling-Brounstein /22/, as well as Dunwald-Wagner /23/ equations, which are listed below.

Jander equation:

$$\frac{2kDt}{r_o^2} = [1-(1-\alpha)^{\frac{1}{3}}]^2 \tag{2}$$

Ginstling-Brounstein equation:

$$\frac{2kDt}{r_o^2} = 1-\frac{2}{3}\alpha-(1-\alpha)^{\frac{2}{3}} \tag{3}$$

Dunwald-Wagner equation:

$$\alpha = 1-\frac{6}{\pi^2}\sum_{n=1}^{\infty}\frac{1}{n^2}\cdot e^{-\frac{n^2\pi^2 Dt}{r_o^2}} \tag{4}$$

In these equations, r_o denotes the radius of the sphere particle; D- the diffusion coefficient; α, k and t respectively stand for the fractional conversion, rate constant and time for the solid-state reaction. The

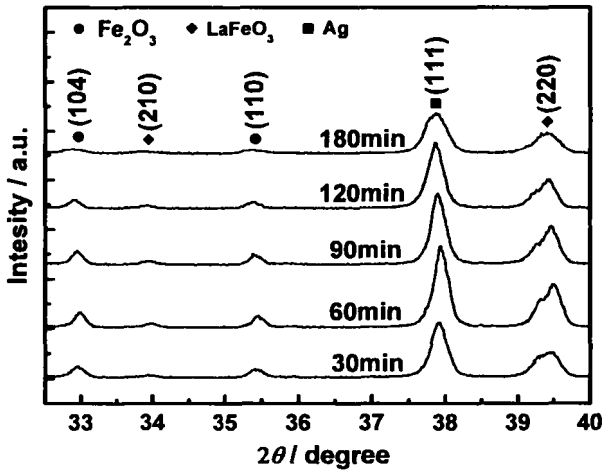

Fig. 3 (a) 1273K

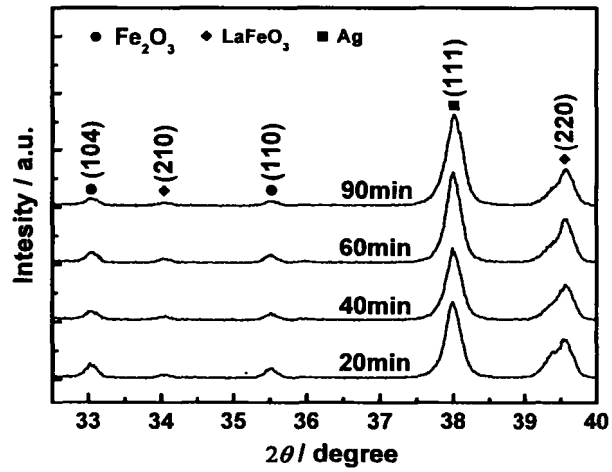

Fig. 3 (b) 1323K

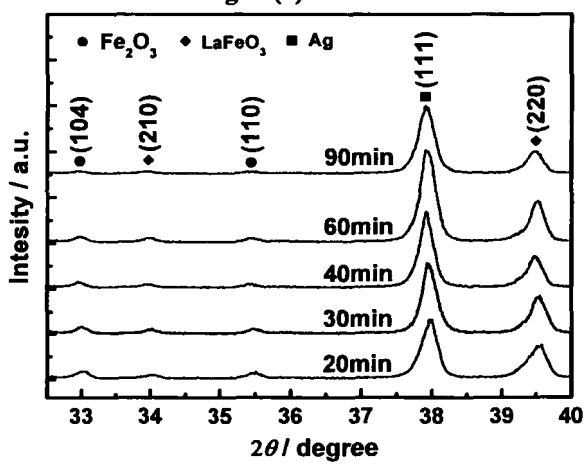

Fig. 3 (c) 1373K

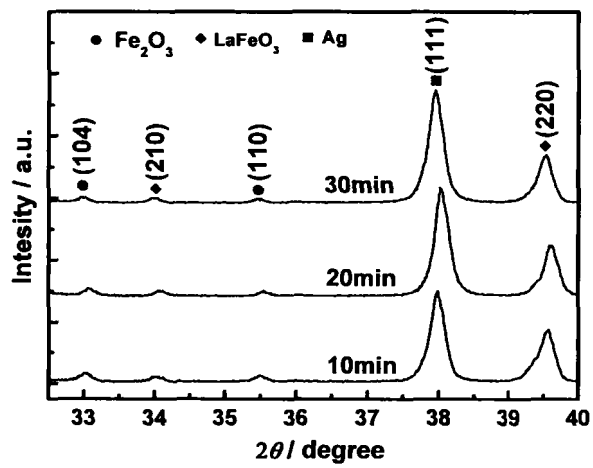

Fig. 3 (d) 1423K

Fig. 3: Part (2θ from 32.4° to 40°) of XRD patterns for composite samples calcined at different temperatures

Table 1

The fractional conversion for different temperature and periods of calcinations

t/min	*T*/K			
	1273	1323	1373	1423
10	-	-	-	0.6824
20	-	0.3490	0.5947	0.7765
30	0.2852	-	0.6707	0.8281
40	-	0.5138	0.7501	-
60	0.3562	0.5927	0.7936	-
90	0.4589	0.7231	0.8635	-
120	0.5517	-	-	-
180	0.6109	-	-	-

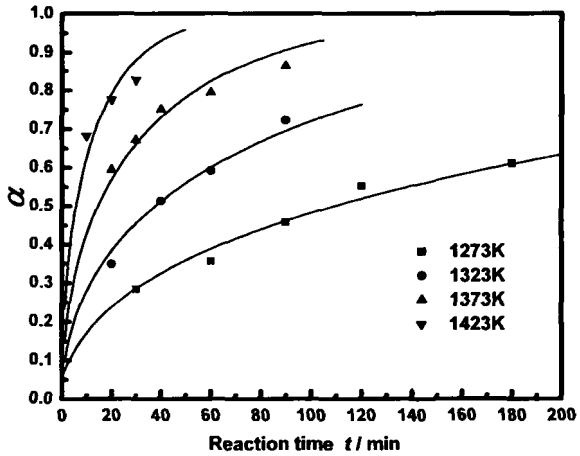

Fig. 4: Relationship between fractional conversions and time, marks: experimental data; solid lines: calculated using Dunwald-Wagner equation

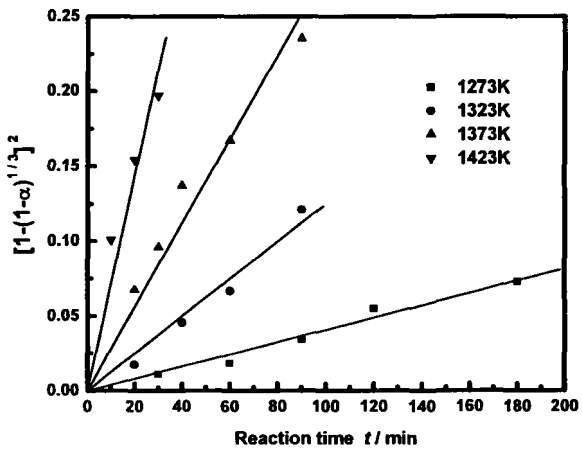

Fig. 5: Jander-fitting to experimental fractional conversions with time

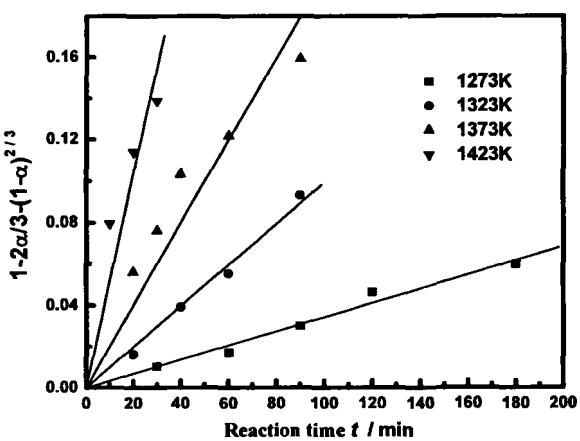

Fig. 6: Ginstling-Brounstein fitting to experimental fractional conversions with time

second term on the right hand side in Eq.(4) is an infinite series. In the present treatment, n=10 was taken to ensure the difference between the limit of the sum of the infinite terms and the sum of the finite ten terms could be smaller than the experimental error for fractional conversion.

Figure 4 demonstrates the Dunwald-Wagner fittings to the experimental data and Figure 5 and Figure 6 show similar fittings using the Jander and Ginstling-Brounstein equations, respectively, for the four experimental temperatures. From Figs. 4~6, one may see that the precisions of the three fittings are commonly good showing the 3D diffusion controlling mechanism. However, Dunwald-Wagner equation follows the reaction better than the Ginstling-Brounstein. Comparing the two linear fittings, it can be seen that the Jander fitting has generated greater correlation coefficient and smaller standard deviation than that of Ginstling-Brounstein fitting mainly at 1373K. The precisions at 1373K obtained from both Jander and Ginstling-Brounstein fittings seem not as better as those at other experimental temperatures. Such a fact has not been found from Fig. 4 for Dunwald-Wagner's fitting. In a previous kinetic study on the formation kinetics for $LaCoO_3$ through solid-state reaction approach, the authors found a similar tendency /13/. The reason still has not been clarified yet, and needs to investigate further.

The above analysis indicates that the three-dimensional diffusion through the product layer was likely to be the rate-controlling step during the overall reaction process.

$\frac{D}{r_0^2}$ values calculated from Dunwald-Wagner equation and the rate constants k obtained from Jander's equation are shown in **Table 2**. The Arrhenius plots using the apparent rate constants k from Jander fitting and $\frac{D}{r_0^2}$ values from Dunwald-Wagner fitting are shown in Figure 7 and Figure 8, and yield apparent activation energies of 282.4kJ/mol and 296.8 kJ/mol respectively. The difference of the two values is reasonably small, and their arithmetic mean value is 289.6 kJ/mol.

Table 2

The rate constant values from Jander fitting and $\frac{D}{r_0^2}$ from Dunwald-Wagner Fitting

T(K)	$\frac{D}{r_0^2}$ (s^{-1}) in Eq. (4)	k (s^{-1}) in Eq. (2)
1273	4.67×10^{-6}	6.80×10^{-6}
1323	1.35×10^{-5}	2.08×10^{-5}
1373	3.50×10^{-5}	4.55×10^{-5}
1423	9.08×10^{-5}	1.19×10^{-4}

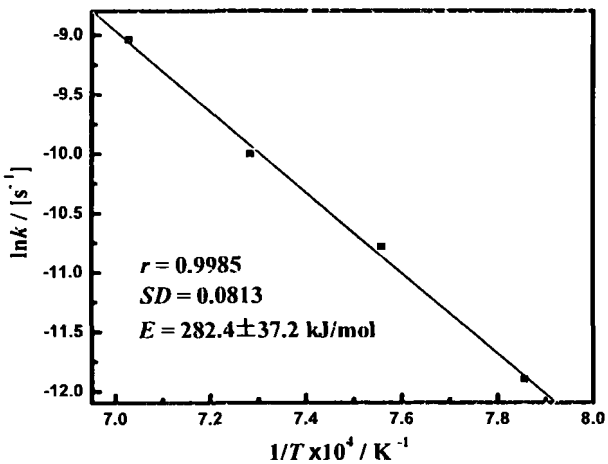

Fig. 7: Temperature dependence of k obtained from Jander fittings

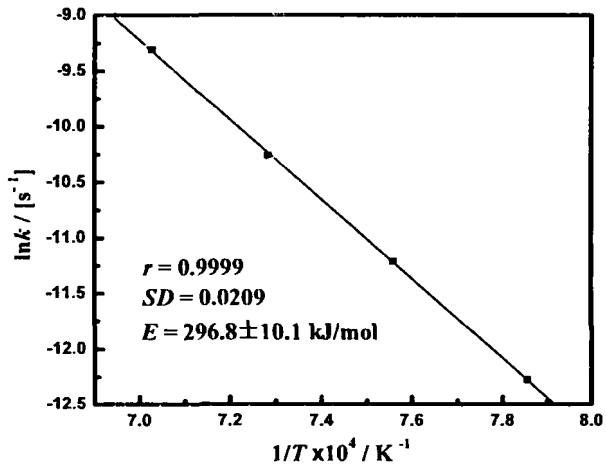

Fig. 8: Temperature dependence of $\frac{D}{r_0^2}$ obtained from Dunwald-Wagner fittings

4. DISCUSSIONS

The experimental results of the present study have shown the solid-ions diffusion controlling mechanism for the overall process of isothermal $LaFeO_{3-\delta}$ synthesis. The concern is which kind of ions, La^{3+}, Fe^{3+} or O^{2-} with the slowest diffusing. The authors have tried to make such a rough estimation from diffusion coefficients of tracer oxygen ions in $LaFeO_{3-\delta}$ single crystal. Ishigaki /24/ measured the tracer diffusion coefficients for oxygen ions, D_O^* in $LaFeO_{3-\delta}$ single crystal between 1173K and 1373K using a gas-solid isotopic exchange technique with ^{18}O tracer, which are listed at the second column of **Table 3**. The following temperature dependence of D_O^* was obtained

$$D_O^*(m^2\cdot s^{-1}) = 2.97\times10^{-7} e^{\frac{214000\pm34000/J\cdot mol^{-1}}{RT}} \quad (5)$$

For comparison, the diffusion coefficients obtained from the present work using Dunwald-Wagner fitting are also shown at the third column of **Table 3**. It can be noted that the diffusion coefficients in the third column are as much as about 1.5 orders less than data at the second one. It can be estimated that the mobility of solid oxygen ions in the $LaFeO_{3-\delta}$ product layer during the heating treatment of the pellets should have been higher than that in the single crystal due to its higher defect density. In such a case, the smaller diffusion coefficients in the third column of **Table 3** may not correspond to the diffusion of solid oxygen ions. This may imply that the diffusion of solid oxygen ions in $LaFeO_{3-\delta}$ product layer may not be the rate-controlling step.

Table 3

Tracer diffusion coefficients of oxygen ions in single crystal $LaFeO_{3-\delta}$ /24/ and diffusion coefficients obtained from Dunwald-Wagner fitting

Temperature/K	D_O^* /m^2·s^{-1}	D /m^2·s^{-1}
1273	4.91×10^{-16}	1.59×10^{-17}
1323	1.05×10^{-15}	4.60×10^{-17}
1273	2.14×10^{-15}	1.19×10^{-16}
1423	4.14×10^{-15}	3.09×10^{-16}

A question that arises is which kind of cation diffusion, lanthanum or iron controlled the solid-state reaction. Obviously no direct evidence was involved in the present experimental study to answer this question. However, it is interesting to compare the present work with a kinetic study on $LaCoO_3$ preparation using solid-state reaction technique /13/. In the previous work, those authors noted the existence of lanthanum vacancies. These vacancies may result in higher valence cobalt, so the movement of cobalt ions is not easier. From the structure of $LaCoO_3$ perovksite, they pointed out that cobalt ions are located in octahedron of oxygen ions, which may limit their mobility. The activation energy for the $LaCoO_3$ formation from solid-state reaction between La_2O_3 and Co_3O_4 233.6 kJ/mol. The value is about 15% lower than that obtained in the present study for $LaFeO_{3-\delta}$. The difference shows that the movement of the cations in $LaFeO_{3-\delta}$ is more difficult, obviously which would be caused by the mobility of iron ion smaller than that of cobalt one. The 2d electron numbers for cobalt and iron are seven and six respectively, and the radii of Co^{3+} and Fe^{3+} are 0.075 and 0.064nm respectively. The smaller radius of Fe^{3+} may indicate strong bonding between Fe^{3+} and oxygen ion. From the above analysis it could be estimated that the diffusion of lanthanum ions in $LaFeO_{3-\delta}$ product layer may be the rate-controlling step in the overall reaction during the isothermal synthesis using the pellet samples.

5. CONCLUSION

The orthorhombic-distorted perovksite of $LaFeO_{3-\delta}$ was synthesized using compacts of solid mixture of La_2O_3 and Fe_2O_3 with two period calcinations each for 8 hrs at 1483K. The lattice parameters obtained through powder XRD measurement were a=0.5553nm, b=0.5561nm, c=0.7842nm, V=0.2422 nm^3.

The kinetic investigation of $LaFeO_{3-\delta}$ formation from compacts of La_2O_3 and Fe_2O_3 powder mixtures under isothermal calcinations carried out at 1273, 1323, 1373 and 1423K provided the following information.

(1) No intermediate product between La_2O_3 and Fe_2O_3 was found during the overall $LaFeO_{3-\delta}$ forming process.

(2) Dunwald-Wagner and Jander equations were adopted to describe the overall reaction process satisfactorily, and producing relevant aarent activation values 282.4 and 296.8 kJ/mol respectively.

(3) The overall reaction process could be controlled by the diffusion of solid-state ions. The diffusion of lanthanum ions through the product $LaFeO_{3-\delta}$ layer may likely be the rate- controlling step.

ACKNOWLEDGEMENT

The financial support for the project 50374008 from National Science Foundation of China is gratefully acknowledged.

REFERENCES

1. S. Nakayama, *Journal of Materials Science*, **36**, 5643-5648 (2001).
2. N. Kimizuka and T Katsura, *Bulletin of the Chemical Society of Japan*, **47**, 1801-1802 (1974).
3. L. W. Tai, M. M. Nasrallah and H. U. Anderson, *Solid State Ionics*, **76**, 259-271(1995).

4. Y. Y. Huang, J. M. Vohs, R. J. Gorte, *Journal of the Electrochemical Society*, **151**, A646-A651(2004).
5. J. A. Lane and S. J. Benson, *Solid Stare Ionics*, **121**, 201-208(1999).
6. A, Petric and P. Huang , *Solid State Inics*, **135**, 715-725(2000).
7. L. Hou, G. F. Sun, K. Liu, Y. Li and F. M. Gao, *Journal of Sol-Gel Science and Technology*, **40**, 9-14(2006).
8. V. R. Choudhary, B. S. Uphade and S. G. Pataskar, *Fuel*, **78**, 919-921(1999).
9. L.Yang, L. S. Wu and L. T. Zhang, *Journal of Alloys and Compounds*, **364**, 83-88(2004).
10. S. G. Li, W. Q. Jin and N. P. Xu, *Solid State Ionics*, **124**, 161-170(1999).
11. W. J. Zheng, R. H. Liu, D. K. Peng and G. Y. Meng, *Materials Letters*, **43**, 19-22(2000).
12. M. Sivakumar, A. Gedanken, W. Zhong, Y. H. Jiang and Y. W. Du, I. Brukental, D. Bhattacharya, Y. Yeshurun, I. Nowik, *Journal of Materials Chemistry*, **14**, 764-769(2004).
13. B. J. Yan, J. Y. Zhang, J. H. Liu, *High Temperature Materials and Processes*, **23**, 163-176(2004).
14. X. P. Dai, C. C. Yu, R. J. Li, Q. Wu, K. J. Shi and Z. P. Hao, *Journal of Rare Earths*, **26**, 341-346(2008).
15. B. J. Yan Baijun, J. Y. Zhang and J. H. Liu, *Journal of Rare Earths*, **22**, 259-262(2004).
16. Q. F. Shu, J. Y. Zhang, J. H. Liu and M. Zhang, *High Temperature Materials and processes*, 24, 169-173(2005).
17. B. J. Yan and J. Y. Zhang, *Z. Metalkunde*, **96**, 902-908(2005).
18. B. J. Yan, J. Y. Zhang and J. H. Liu and G. R Liu, *Materials Letters*, **59**, 3226-3229(2005).
19. Q. F. Shu, J. Y. Zhang, J.H. Liu, *Journal of Alloys and Compounds*, **390**, 240-244(2005).
20. B. F. Chung, *J. Alied Crystal*, **7**, 519-525 (1974).
21. W. Jander, *Z. Anorg. Allg. Chem.*, **163**, 1-30(1927).
22. A. M. Ginstling and B. J. Brounshtei, *J. Al. Chem. USSR*, **23**, 1327-1328(1950).
23. H. Dunwald and C. Wagner, *Z. Physik. Chem.*, **B24**, 53-58(1934).
24. T. Ishigaki, S. Yamauchi and J. Mizusaki, *J. Solid State Chem.*, **55?**, 50-53(1984).